Report

Cell Reports

Amino acid formula induces microbiota dysbiosis and depressive-like behavior in mice

Graphical abstract

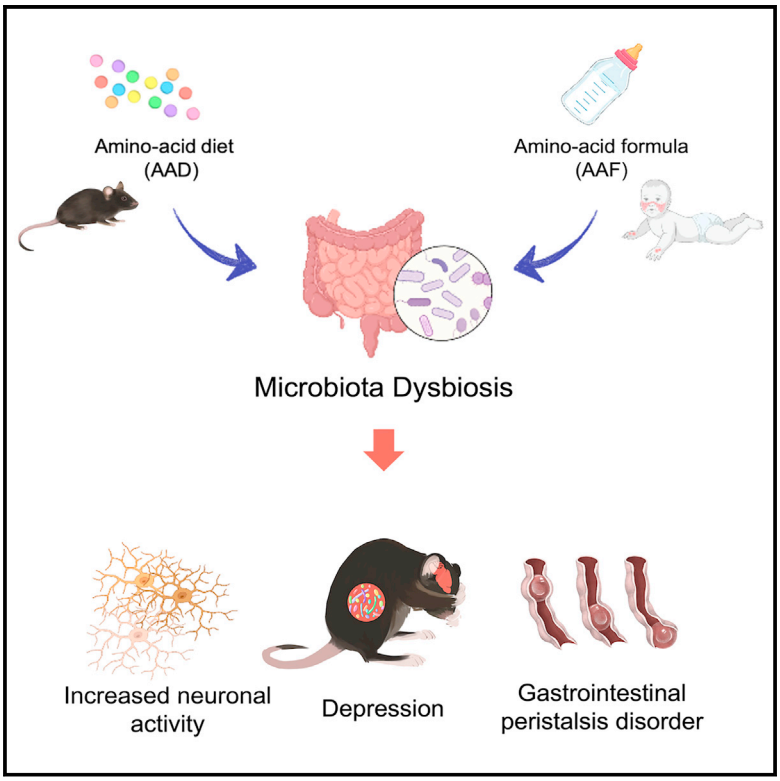

Authors

Ji Hu, Kaixin He, Yifei Yang, ..., Guoqiang Bi, Lan Zhang, Shu Zhu

Correspondence

zhanglan1978@ustc.edu.cn (L.Z.), zhushu@ustc.edu.cn (S.Z.)

In brief

Hu et al. report amino acid diet (AAD)- and amino acid formula (AAF)-induced behavioral changes in mice with elevated neuronal activation, regulated by gut microbiota. This underscores valuable insights into potential links between AAF-fed children and mental well-being.

Highlights

- AAD feeding leads to depressive-like behavior and GI motility disorder in mice
- AAD feeding leads to increased neuronal activities
- AAD-feeding-induced behavioral changes are microbiota dependent
- FMT from AAF-fed infants leads to depressive-like behavior in GF mice

Hu et al., 2024, Cell Reports *43*, 113817
March 26, 2024
https://doi.org/10.1016/j.celrep.2024.113817

CellPress

Cell Reports

CellPress
OPEN ACCESS

Report

Amino acid formula induces microbiota dysbiosis and depressive-like behavior in mice

Ji Hu,[1,2,4] Kaixin He,[1,2,4] Yifei Yang,[3] Chuan Huang,[1] Yiping Dou,[1] Hao Wang,[1] Guorong Zhang,[1,2] Jingyuan Wang,[1] Chaoshi Niu,[2] Guoqiang Bi,[1] Lan Zhang,[2,*] and Shu Zhu[1,2,3,5,*]

[1]Key Laboratory of Immune Response and Immunotherapy, Center for Advanced Interdisciplinary Science and Biomedicine of IHM, School of Basic Medical Sciences, Division of Life Sciences and Medicine, University of Science and Technology of China, Hefei, China
[2]The First Affiliated Hospital of USTC, University of Science and Technology of China, Hefei, China
[3]School of Data Science, University of Science and Technology of China, Hefei, China
[4]These authors contributed equally
[5]Lead contact
*Correspondence: zhanglan1978@ustc.edu.cn (L.Z.), zhushu@ustc.edu.cn (S.Z.)
https://doi.org/10.1016/j.celrep.2024.113817

SUMMARY

Amino acid formula (AAF) is increasingly consumed in infants with cow's milk protein allergy; however, the long-term influences on health are less described. In this study, we established a mouse model by subjecting neonatal mice to an amino acid diet (AAD) to mimic the feeding regimen of infants on AAF. Surprisingly, AAD-fed mice exhibited dysbiotic microbiota and increased neuronal activity in both the intestine and brain, as well as gastrointestinal peristalsis disorders and depressive-like behavior. Furthermore, fecal microbiota transplantation from AAD-fed mice or AAF-fed infants to recipient mice led to elevated neuronal activations and exacerbated depressive-like behaviors compared to that from normal chow-fed mice or cow's-milk-formula-fed infants, respectively. Our findings highlight the necessity to avoid the excessive use of AAF, which may influence the neuronal development and mental health of children.

INTRODUCTION

Extensively hydrolyzed formula (EHF) and amino acid formula (AAF) are increasingly recommended for infants with cow's milk protein allergy (CMPA), depending on the severity of their CMPA.[1,2] The prevalence of CMPA in developed countries ranging from 0.5% to 3% at age 1 year[3,4]; however, the prescription of EHF and AAF, especially AAF, increased 6.7-fold during 2007–2018 and accounted for 55% of expenditure on the costs of specialized formula in England, Norway, and Australia,[5] suggesting potential overdiagnosis of milk allergy and excessive use of AAF in these countries.[6,7] The side effects of AAF have been studied in relation to dental decay and obesity[8–10]; however, the specific effects of AAF on neuronal development and mental health remain poorly understood.

Major depressive disorder (MDD) is a debilitating mental illness associated with significant morbidity and mortality.[11] The precise etiology of depression is multifactorial and involves complex signaling networks, and lifestyle factors like diet, sleep, and exercise have been supposed to be associated with MDD.[12,13] Dietary patterns have also been reported to regulate microbiota.[14,15] The gut microbiota has been recognized as a key factor in modulating brain function and behavior in the communication of gut and brain,[16] and accumulating evidence from preclinical and clinical studies have suggested the potential role of gut microbiota in the pathophysiology of depression.[17]

We have used amino acid diet (AAD) feeding as a mouse model to study how feeding without intact protein breaks immune tolerance to food.[18] Occasionally, we found that these AAD-fed mice developed depressive-like behavior, leading to the concern of the long-term mental health for those AAF-fed infants. We discovered that AAD led to depressive-like behavior in mice, with gut microbiota dysbiosis and neuronal activation as measured by 16S and whole-brain cFos imaging. Infants fed with AAF exhibit microbiota dysbiosis,[19] and fecal from AAF-fed infants transplanted into germ-free (GF) mice also led to the depressive-like behavior. Taken together, our study indicates a potential risk in infants with AAF, as their microbiota dysbiosis could contribute to mental disorders with increased neuronal activities.

RESULTS

AAD induces depressive-like behavior in mice

To mirror the situation of infants with AAF, we generated a mouse model feeding with AAD (Figure 1A). The AAD is a chemically defined elemental diet devoid of macromolecules, as previously been reported[20,21] (Tables S1 and S2). Neonatal mice were divided into two groups, simultaneously fed with normal chow diet (NCD) or AAD. After feeding for 4 weeks, the AAD-fed group was switched to an NCD to closely mimic the transition from AAF to regular formula in clinical practice. At the age of 6 weeks, we assessed the general behaviors

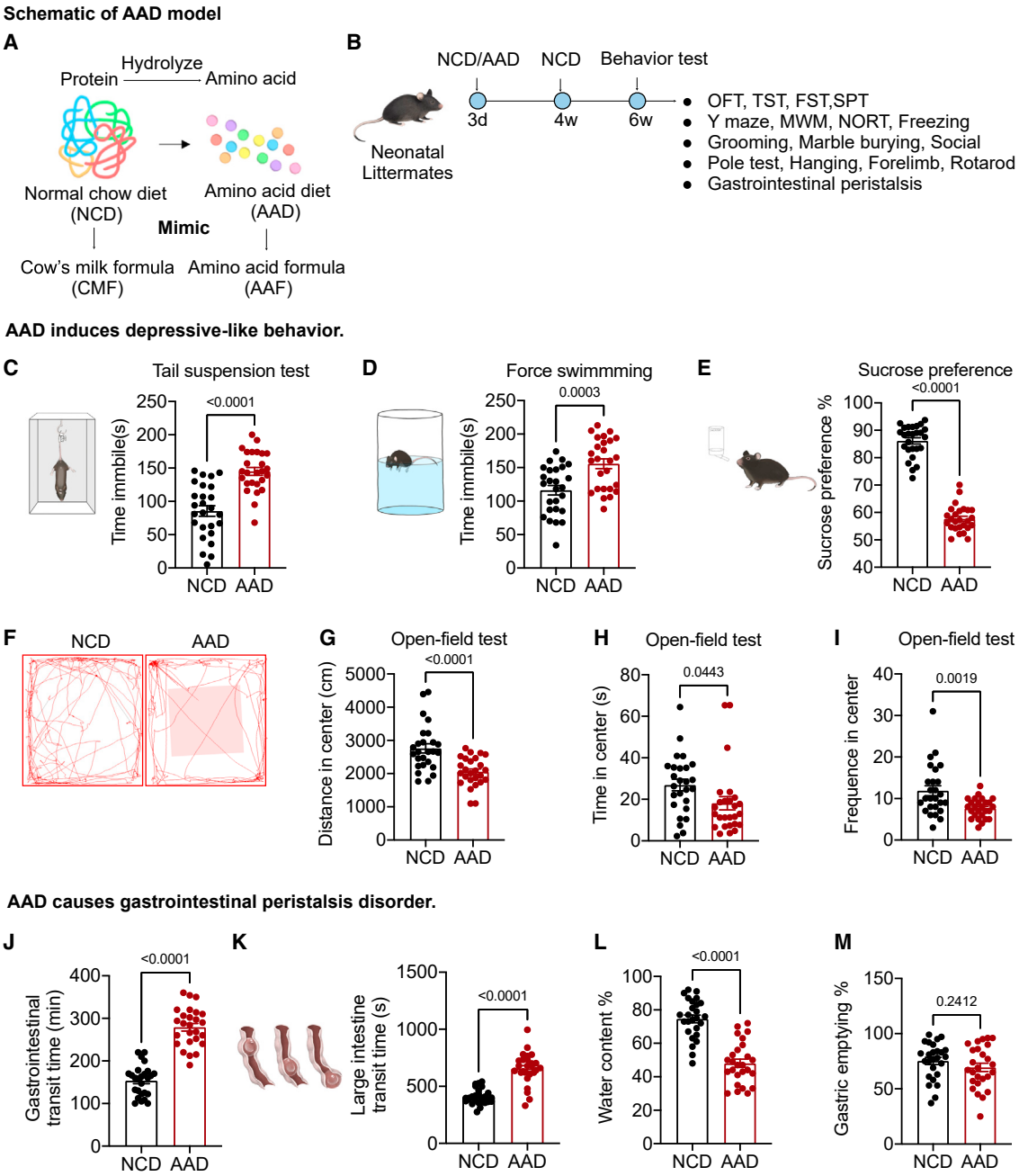

Figure 1. Amino acid diet (AAD) induces depressive-like behavior and gastrointestinal peristalsis disorder in mice

(A) Schematic of AAD.

(B) Neonatal littermates C57/B6J mice were fed with normal chow diet (NCD) or AAD from the age of 3 days to 4 weeks and the AAD-fed group was switched to NCD; at the age of 6 weeks, the mice took behavior tests and GI motility tests.

(C and D) The immobility (immobile time per minute) of the mice in the TST and FST between NCD- and AAD-fed groups.

(E) The preference for sucrose (amount of sucrose consumed/total water intake in 24 h) of the mice between NCD- and AAD-fed groups.

(F–I) Representative tracks of NCD- or AAD-fed mice in open-field test (OFT), as well as (G) travel distance, (H) time spent in center, and (I) frequency into center.

(J) Whole-gut transit time between NCD- and AAD-fed groups.

(K) Bead latency test to measure colon transit time.

(L) Water content of the feces from NCD- and AAD-fed mice.

(M) Gastric emptying test to measure the time taken for ingested food to leave the stomach and move into the small intestine.

For (C)–(M), data are mean ± SEM, as determined by two-tailed paired t test, n = 26.

See also in Figure S1.

and physiological conditions of the gut and brain between the two groups (Figure 1B). AAD-fed mice appeared to be of similar size and body weight to NCD-fed mice (Figure S1A). The morphology, colon lengths, and histology of the intestine between the two groups appeared no different (Figure S1B–S1F). We also measured the energy consumption of AAD and NCD mice, and the results showed no differences in food and water intake (Figure S1G–S1H). Interestingly, these AAD-fed mice exhibited depressive-like behaviors, presenting as increased immobility in the forced swimming test (FST) and the tail suspension test (TST) without changes in overall locomotor activities, and decreased preference in the sucrose preference test (SPT) without altered total consumption (Figures 1C–1E). Moreover, in contrast to NCD-fed mice, AAD-fed mice exhibited reduced interest in exploring the central region and reduced locomotion in the open-field test (Figures 1F–1I), showing that these mice exhibit more anxiety.

However, there were no significant differences between the two groups in other behavioral tests, including the Morris water maze test, Y-maze test, rotarod test, grip strength test, hanging test, pole test, and freezing time (Figures S1J–S1S), implying that AAD feeding did not affect the cognition and motility of mice. Social behavior in the novel object recognition test (NORT), grooming test, marble burying, and social interaction (Figures S1T–S1X) reflected no differences between AAD- and NCD-fed mice. Since increased corticotropin-releasing hormone was postulated to be the indicator of depression,[22,23] we consistently found that AAD-fed mice had significantly increased levels of corticosterone compared to NCD-fed mice (Figure S1I). Collectively, these data demonstrate that AAD feeding induces depressive-like behavior in mice.

AAD induces gastrointestinal (GI) peristalsis disorder in mice

Besides the depressive-like behavior controlled by the central nervous system (CNS), we also explored the direct impact of AAD feeding on the GI tract's function controlled by the enteric nervous system (ENS). Peristaltic movements of the gut are essential to facilitate proper anterograde propulsion of luminal contents.[24] In AAD- and NCD-fed mice, we assessed the whole intestinal transit time, which measures GI motility from the time food enters the stomach until it is removed from the body as waste. Curiously, AAD-fed mice exhibited significantly higher intestinal transit times compared to NCD-fed mice (Figure 1J), requiring about 280 min to expel the carmine fecal pellet compared to 150 min for NCD-fed mice. To gain a more precise understanding of the specific region of the intestine affected, we next evaluated regional motility by measuring gastric emptying and colon transit time. We found that AAD-fed mice had increased colon transit times compared to NCD-fed mice (Figure 1K), with lower fecal water content in the feces of AAD-fed mice (Figure 1L). However, the gastric emptying test showed no differences between the two groups (Figure 1M). Taken together, the results showed that while the times taken for different foods to enter the small intestine are similar in both groups, AAD-fed mice exhibit increased GI peristalsis disorder.

Increased cFos activation in the whole brain and gut of AAD mice

The expression of immediate-early genes (IEGs) corresponds to the activation of specific circuitry of the brain related to perception and integration of primary stimuli as well as to autonomic and behavioral responses.[25] Immobilization stress for 30 min can induce intense expression of cFos (and other IEGs) in several brain areas.[26] However, the effects of AAD-feeding-induced neuronal activities have not been assessed. Therefore, we conducted whole-brain mapping of neuronal activity in AAD- and NCD-fed mice by evaluating the cFos expression. We employed a sample-preparation strategy with tissue clearing and staining 300 μm slices and reconstructed the whole-brain image by using Imaris v.9.8 (bitplane, Oxford Instruments) (Videos S1 and S2). We counted the number of cFos activated neurons with a semi-automated procedure (Figure 2A). Staining intensity of individual cFos-positive cells varied from very intense (black) to very light (light brown). Overall, we observed a robust increase of cFos expression throughout the whole brain of AAD-fed mice compared to NCD-fed mice (Figure 2B). We further quantified cFos-expressing neurons by staining serial section with 50 μm slices, and by comparing the example images of the forebrain, midbrain, and hindbrain in the two groups, we confirmed a reliable induction of cFos activation in the forebrain, midbrain, and hindbrain, with an increased number of cFos-positive cells in AAD-fed mice (Figures S1Y and S1Z). In addition to the brain, we also measured the potential influence of AAD feeding on the sympathetic neurons, as we observed GI peristalsis deficits in these mice. Immunofluorescence analysis showed that AAD-fed mice exhibited significantly more positive cFos neuronal nuclei in the colon compared to NCD-fed mice (Figures 2C and 2D). Collectively, these data suggest that AAD feeding contributes to elevated levels of sympathetic activity in both the CNS and ENS.

AAD-induced depressive-like behavior is independent of vagus nerve or immune-mediated gut-brain connection

To delve deeper into the mechanisms behind AAD-feeding-induced depressive-like behavior, we examined both direct and indirect dietary pathways leading to mental disorders. The vagus nerve is recongnized as a neuronal pathway linking the gut and brain.[27] To evaluate whether AAD-feeding-induced depressive-like behavior is regulated by the vagus nerve, subdiaphragmatic vagotomy (sdVx) was conducted in AAD-fed mice. The sdVx was performed by cutting the left and right vagal nerves along the esophagus, and the size and weight of stomach were recorded to confirm a successful sdVx (Figures S2A–S2C). After surgery, the mice were fed with AAD and NCD for 4 weeks and behavior tests were conducted. The results showed no differences in TST, FST, SPT, and intestinal transit time across the groups of sdVx, sham-operated, and non-treated mice (Figures S2D–S2G), which demonstrated that the AAD-feeding-induced depressive-like behavior is not regulated via the vagus nerve.

Previous studies have established that a high-cholesterol diet can lead to disruption of the blood-brain barrier (BBB) in mice, consequently resulting in cognitive impairments.[28] In light of

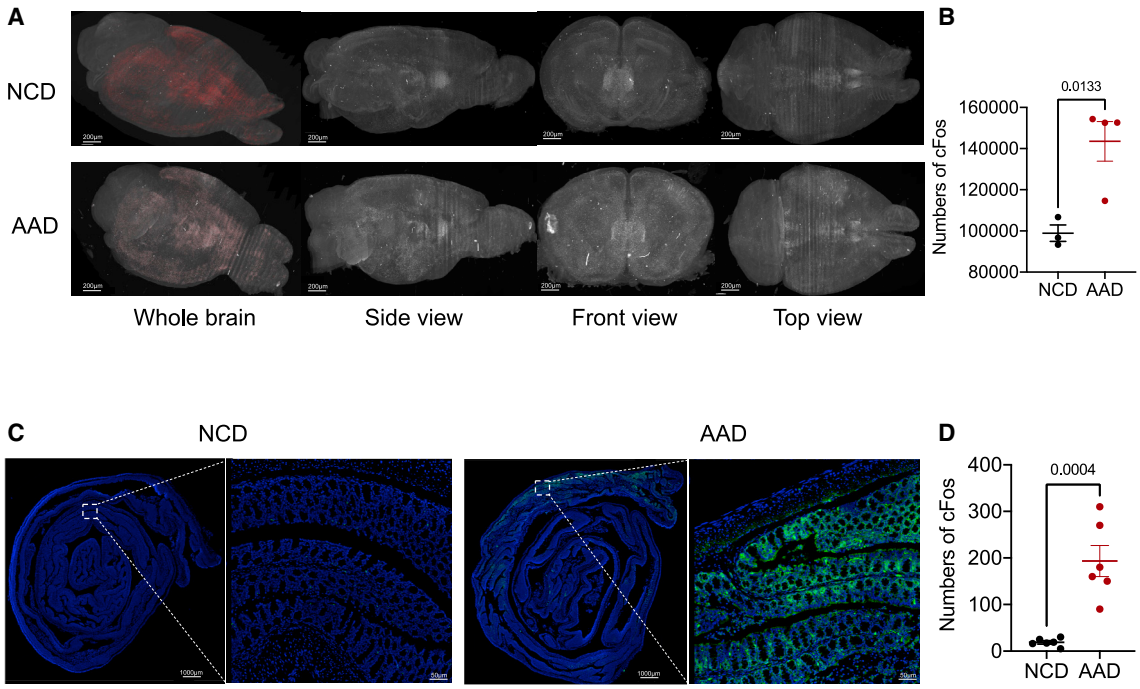

Figure 2. Increased cFos activation in the whole brain and colon in AAD-fed mice

(A) Brain-wide cFos imaging of AAD- and NCD-fed mice (from left to right, 3D-reconstructed mouse brain, side view, front view, top view).

(B) The number of cFos-expressing neurons in the whole-brain imaging (NCD n = 3, AAD n = 4).

(C) cFos staining in the colon of NCD- and AAD-fed mice.

(D) The number of cFos-expressing neurons in the colon (n = 6).

For (B) and (D), data are mean ± SEM, as determined by two-tailed paired t test.

See also in Figure S1.

these findings, we assessed the permeability of the BBB in mice subjected to NCD and AAD feeding. We found no alterations in BBB permeability between AAD-fed and control mice as measured by 2% Evans blue dye in the brain after intravenous injection. The result suggests that the AAD feeding does not affect the permeability of the BBB (Figure S2H).

Further, the immune system, acknowledged as a significant modulator of animal behaviors, was also evaluated.[29] To examine the role of the immune system in AAD-feeding-induced behavioral changes, we exposed *recombination activating gene 1* (*Rag1*$^{-/-}$) mice and wild-type (WT) mice to AAD for 4 consecutive weeks and then measured the mice's depressive-like behavior (Figure S2I). Immunodeficient *Rag1*$^{-/-}$ mice and WT mice exhibit similar behaviors: increased immobility in the FST and TST, decreased preference in the SPT, and higher gut transit time (Figures S2J–S2M). This implies that lymphocyte migration is less likely to contribute to the AAD-induced depressive-like behavior.

Together, these results suggest that neither the vagus nerve- nor the immune system-mediated gut-brain connection plays a pivotal role in AAD-induced depressive-like behavior.

AAD induced depressive-like behavior in a microbiota-dependent way

Since it is known that AAF induces the dysbiosis of the microbiota[19,30] and that microbiota transplantation from patients with MDD to rodents leads to depression-like behaviors,[19,31,32] we reasoned that the aforementioned phenotype we observed might due to the microbiota dysbiosis. We analyzed the bacterial composition and community structure in the feces of AAD- or NCD-fed mice by 16S ribosomal RNA (rRNA) gene sequencing. The α-diversity of microbiota in AAD-fed mice was significantly reduced compared to that in NCD-fed mice (Figure 3A). Bacterial diversity computed based on weighted UniFrac distances (the assessment of community structure by considering abundance of operational taxonomic units) revealed a significant difference between the AAD- and NCD-fed mice (Figure 3B). We observed shifted microbial communities in AAD-fed mice (Figure 3C), with significant lower abundance of the phylum *Firmicutes*, such as *Clostridia,* and the order *Bacteroidales*, such as *Prevotellaceae* and *Muribaculaceae* (Figures S3A–S3E), as well as higher levels of the phylum *Actinobacteriota*, such as *Corynebacteriaceae, and Deferribacterales* (Figures S3F–S3H). Collectively, these data showed that the AAD feeding altered the composition of gut microbiota.

Then, we tested the minimum AAD-feeding period that is sufficient to alter microbiota community. We monitored the microbial community changes from the first to the sixth week during the AAD feeding and also recorded the depressive-like behavior and GI motility. We found that the Shannon index (quantitative measure of community richness) increased continuously with age and that AAD-fed mice harbored decreased α-diversity of

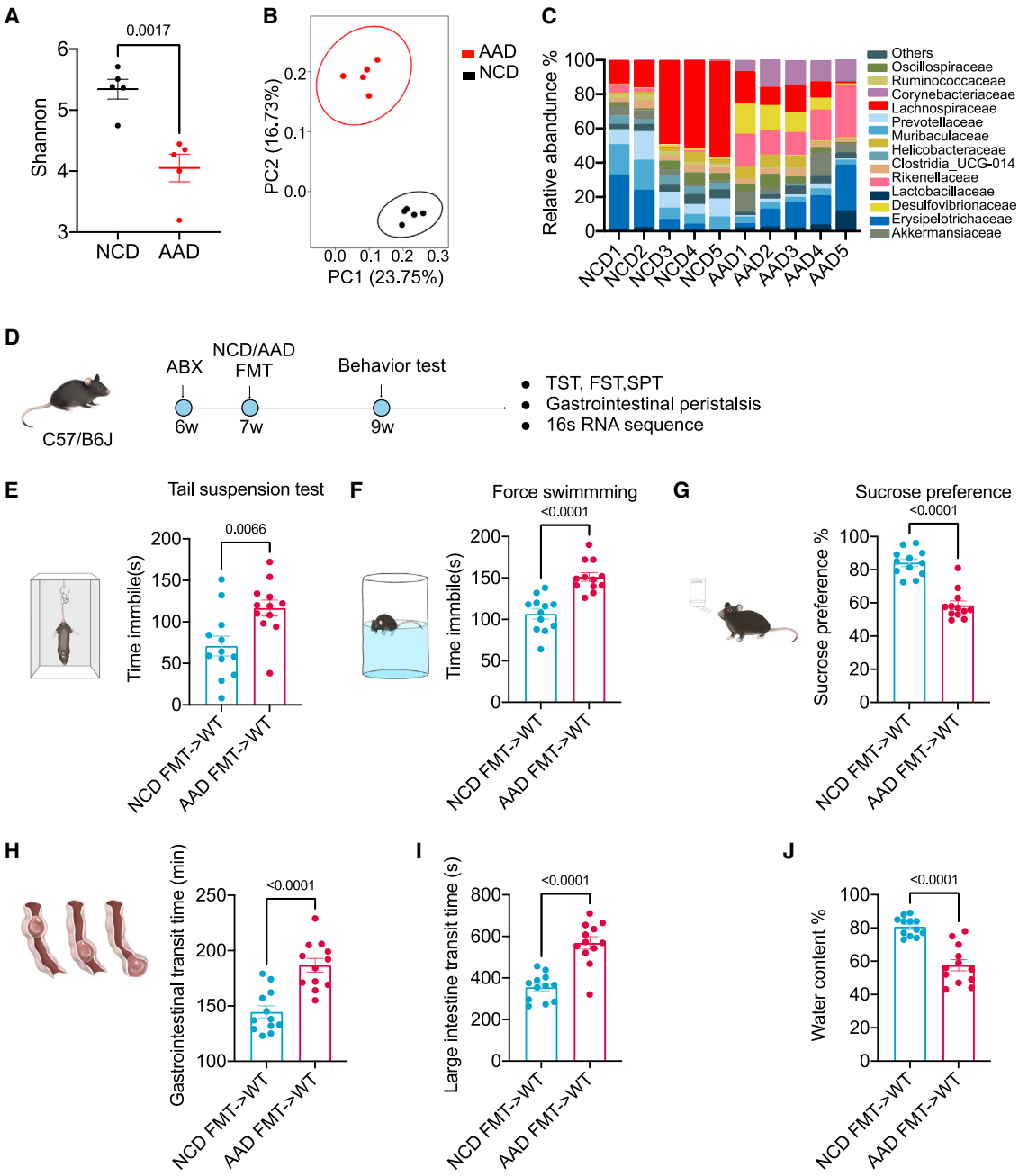

Figure 3. The gut microbiota regulates AAD-feeding-induced depressive-like behavior and gastrointestinal peristalsis disorder

(A–C) 16S rRNA sequencing of the feces from AAD- and NCD-fed mice.

(A) Estimation of microbial community α-diversity (observed Shannon) between AAD- and NCD-fed groups (n = 5).

(B) Principal-component analysis (PCA) plot generated from an unweighted UniFrac distance matrix displaying the distinct clustering pattern of the intestinal bacteria community for AAD- and NCD-fed groups (n = 5).

(C) Relative abundance data for gut microbiota (family-level taxonomy) are presented as a percentage of the total detected sequences.

(D) Schemata of experimental design: C57/B6J mice were orally administered with antibiotics for 7 days, following FMT for 2 weeks, and then we conducted behavior tests and GI motility.

(E–G) Depressive-like behavior tests after FMT (n = 12), (E) TST, (F) FST, and (G) SPT between FMT-recipient mice.

(H–J) GI motility tests after FMT (n = 12).

(H) Whole-gut transit time.

(I) Bead latency test to measure colon transit time.

(J) Water content of the feces from FMT recipient mice. NCD FMT→WT, NCD's feces transferred to WT; ACD FMT→WT, AAD's feces transferred to WT.

For (A) and (E)–(J), data are mean ± SEM, as determined by two-tailed paired t test, ns, no significance.

See also in Figure S3.

microbiota as early as the first week of AAD exposure (Figure S3I). The principal coordinates analysis of microbiota was also performed over a time course in fecal samples of NCD- and AAD-fed mice (Figure S3J), and the differences persisted throughout the AAD treatment (Figure S3K). Increased immobility of TST was observed starting from the fourth week post-AAD feeding and reached a significant change in the sixth week (Figure S3L). An increasing trend of colon transit times in the AAD-fed group was also observed starting from the second week after AAD exposure (Figure S3M). Thus, AAD feeding leads to the microbiota alteration in only 1 week, triggers GI motility dysfunction beginning at 2 weeks, and induces depressive-like behavior from 6 weeks.

We next performed fecal microbiota transplantation (FMT) to test whether the altered gut microbiota is responsible for the depressive-like behavior and GI peristalsis phenotype (Figure 3D). Fecal microbiota from AAD- or NCD-fed mice were transferred by oral gavage into antibiotics-treated WT mice in C57/B6J background (AAD FMT→WT and NCD FMT→WT). After 2 weeks of colonization, microbiota transferred from AAD-fed mice (AAD FMT→WT) led to increased immobility in the FST, TST, and SPT (Figures 3E–3G), indicative of depressive-like behavior. FMT from AAD-fed mice (AAD FMT→WT) increased the colon transit time and whole-gut transit time in recipient mice (Figures 3H and 3I), as well as lowered the water contents of feces (Figure 3J), indicative of GI peristalsis disorder.

Sequencing of the 16S rRNA verified the microbiota reconstitution in the recipient mice. When comparing the microbial structures of recipient and donor mice, the microbial composition in AAD FMT→WT recipient mice is similar to that of AAD-fed mice. Likewise, the microbial makeup of NCD FMT→WT recipient mice is closer to that of NCD-fed mice than other groups (Figures S3N and S3O). A heatmap showcasing the relative abundance of family-level taxa like *Bacteroides*, *Faecalibacterium*, *Lachnospiraceae*, *Ruminococcaceae*, *Muribaculaceae*, *Lachnospiraceae*, and *Clostridia_UCG-014* across each group underscores this similarity (Figure S3Q). The bacterial species compositions between two recipient groups are also different (Figures S3R and S3S). Consistent with the enhanced depressive-like behavior, we detected an increased level of corticosterone in the serum of AAD FMT→WT group (Figure S3P). We also examined cFos expression in FMT mice; according to whole-brain imaging, the AAD FMT→WT mice showed stronger cFos activation in the forebrain compared to NCD FMT→WT mice (Figures S3T and S3U). These data demonstrate that AAD-induced microbiota dysbiosis contributes to the depressive-like behavior and GI peristalsis disorder.

FMT of AAF-fed infants leads to depressive-like behavior in GF mice

Since previous studies showed that AAF-fed infants also showed altered microbiota,[19] we next sought to determine whether microbiota from AAF-fed infants also tend to induce depressive-like behavior. We performed an integrated analysis of the gut microbiota from AAF-fed (32) and cow's milk formula (CMF)-fed (28) Asian children (Figure S4A). Principal-component analysis on the basis of genus composition revealed profound differences between the two groups (Figure 4A). Besides, the microbiota of AAF-fed children showed decreased α-diversity compared to CMF-fed children (Figure 4B). The linear discriminant analysis effect size (LEfSe) analysis showed the bacterial differences between the two groups (Figures 4C and 4D), including increased levels of *Actinobacteriota* (phylum) (Figure S4B), which corresponded to the changes in AAD- vs. NCD-fed mice. Other than that, levels of *Enterobacterales*, *Enterobacterales* (order), and *Gammaproteobacteria* (class) were higher, and levels of *Deferribacterales* (order) were lower, in the feces of AAF-fed children as compared to the CMF-fed group (Figures S4C–S4C).

Additionally, we sought to determine whether the commonly used AAFs (Nestle Alfamino) could directly cause depressive-like behaviors in mice (Figure S4G). Interestingly, mice fed with AAF exhibited depressive-like behaviors similar to those noted in our other studies, with significant increases in immobility during the FST and TST, decreased preference in the SPT, and an elevated gut transit time when compared to those fed with CMF (Nestle Beba) (Figures S4H–S4K).

To investigate whether FMT from AAF-fed infants could induce a depressive-like phenotype in mice, we performed FMT from 3 donor infants fed with AAF for 3, 4, and 5 months (FMT-AAF1, -AAF2, and -AAF3, respectively) and 2 donor CMF individuals (FMT-CMF1 and -CMF2, respectively) into GF mice and then assessed the depressive-like behaviors (Figure 4E). According to the results, there was a tendency toward higher immobility in the TST weeks post-transplantation in FMT-AAF mice (Figures 4F and 4G). Transplantation of AAF2 and AAF3 to GF mice caused a significant increase of immobile time compared to CMF1-transferred GF mice. FMT-AAF mice also displayed decreased preference for sugar water in the SPT (Figures 4H and 4I). We also detected the corticosterone levels in the serum from individual CMF1- and AAF3-transferred GF recipient mice and confirmed a higher level of corticosterone in FMT-AAF3 mice compared to FMT-CMF3 mice (Figure S4F). Furthermore, we analyzed the cFos activation in the FMT-AAF3 and FMT-CMF1 mice. The whole-brain cFos staining showed significantly stronger neuronal activation in FMT-AAF3 mice than in FMT-CMF3 mice (Figures S4L and S4M). Taken together, we found that microbiota from AAF-fed infants also tend to induce depressive-like behavior in mice.

DISCUSSION

Dietary patterns have been shown to influence mental health, and meta-analyses showed cross-sectional and prospective associations between diet quality and mental health.[33,34] Evidence from observational studies suggests that diets enriched in plant foods, such as vegetables, fruits, legumes, and whole grains, and lean proteins, including fish, are associated with a reduced risk for depression, while dietary patterns that include more processed food and sugary products are associated with an increased risk of depression.[12] A dose-dependent relationship between dietary fiber intake and risk of depression has also been reported.[35] However, the association between the widespread use of AAF and the risk of depression has not been investigated. We conducted animal models to find that AAD-fed mice

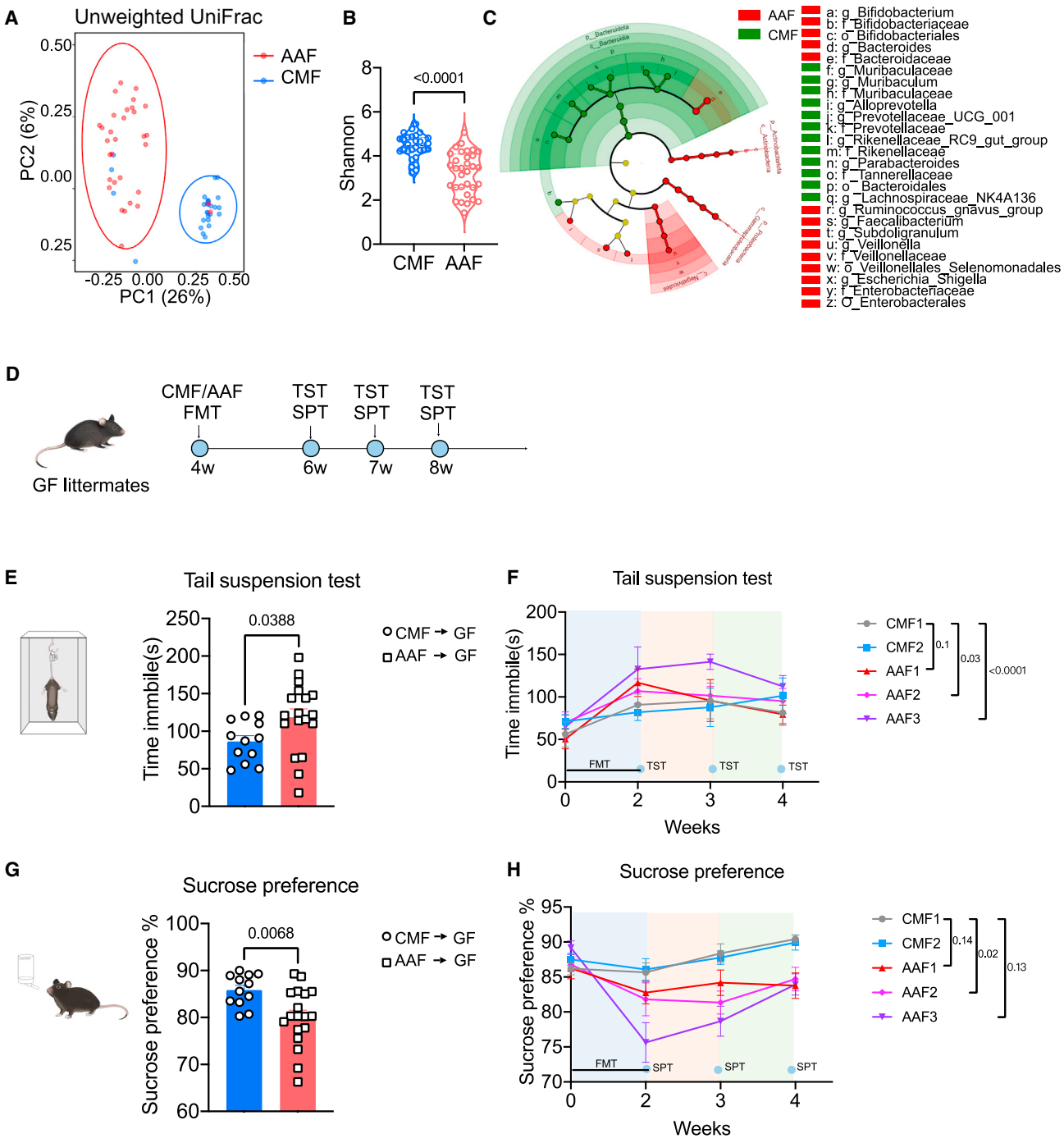

Figure 4. Fecal microbiota of AAF-fed children leads to depressive-like behavior in GF mice

(A–D) Fecal samples were collected from CMF- (n = 28) and AAF-fed (n = 32) children for 16S rRNA sequencing.

(A) PCA plot generated from an unweighted UniFrac distance matrix displaying the distinct clustering pattern of the intestinal bacteria community for CMF- and AAF-fed groups.

(B) Estimation of microbial community α-diversity (observed Shannon).

(C) LEfse analysis between CMF- and AAF-fed groups.

(D) Schematic of FMT of feces from 2 CMF-fed individuals into GF mice (n = 12) and 3 AAF-fed individuals transferred into GF mice (n = 18).

(E–H) TST (E and F) and SPT (G and H) of FMT mice.

For (B), (E), and (G), data are mean ± SEM, as determined by two-tailed paired t test. For (F) and (H), data are mean ± SEM, as determined by two-way analysis of variance (ANOVA), ns, no significance.

See also Figures S6 and S4.

exhibit depressive-like behavior, providing the causation between AAF feeding and mental health.

Dietary components play a crucial role in shaping the gut microbiota, as different dietary amino acids can profoundly impact the function of gut microbes.[14,15,36] Previous studies have reported that infant formulas such as AAF alter the gut microbiota in children[19,37]; however, the exact process of microbiota regulation during AAF feeding is not known. We monitored the microbiota as well as the depressive-like behavior during 6 weeks of the AAD feeding in mice. We observed significant changes in microbiota upon feeding with AAD for only 1 week; we found that mice fed with an AAD for 2 weeks develop GI peristalsis disorder, and mice fed for 6 weeks start to develop depressive-like behavior. These results indicate that the establishment of the neonatal microbiota is of great importance for long-term neuronal development and mental health.

It is reported that the extended use of AAF increased the potential risk in several disease, such as dental decay and obesity.[1,30] Two large cohort studies revealed allergic disorder in early childhood (a population with potential higher usage of EHF) significantly increased the risk of autism spectrum disorder or attention-deficit hyperactivity disorder.[38,39] However, a direct link between the use of AAF and psychological problems such as depression is still lacking experimentally or clinically. Based on our findings, we provide animal experimental data to support the potential influence of AAF feeding on the development of depressive-like behavior. When considering the clinical prescription for food allergy in formula-taken infants, first of all, try to avoid using AAF; second, try to minimize the use of the EHF. For food allergy in breastfed infants, at first, try not to discontinue the breastfeeding but avoid the suspected allergens; second, if it is still not better, try EHF for 2–4 weeks. Once the food allergy improves, stop EHF feeding and switch back to cow's milk or breastfeeding, to reduce the potential risk for developing mental disorder.

Limitations of the study

Two questions may need further investigations. First, how does microbiota dysbiosis induced by AAD/AAF feeding contribute to the depressive-like behavior in mice? Second, do our findings suggesting a potential risk of mental disorders in infants fed with AAF necessitate prospective studies on mental health within AAF-fed cohorts to establish the link between AAD-fed in infancy and depression?

STAR★METHODS

Detailed methods are provided in the online version of this paper and include the following:

SUPPLEMENTAL INFORMATION

Supplemental information can be found online at https://doi.org/10.1016/j.celrep.2024.113817.

ACKNOWLEDGMENTS

We thank Dr. Hongdi Ma for helpful discussions. We thank Chunhui Jia for cFos whole-brain reconstruction. We would like to acknowledge the Multimodality Imaging Center of the Institute of Artificial Intelligence of Hefei Comprehensive National Science Center for the whole-brain VISoR imaging and L. Guo and W. Zheng for their assistance in data collection and analysis. This work was supported by grants from the National Natural Science Foundation of China (82325025) (S.Z.) and the CAS Project for Young Scientists in Basic Research (YSBR-074) (S.Z.).

AUTHOR CONTRIBUTIONS

J.H. and K.H. designed the experiments. J.H. performed and interpreted most of the experiments. Y.Y. analyzed the 16S data. H.W. and Y.D. performed the cFos staining assay. C.H. reconstructed the whole-brain image. G.Z. and J.W. conducted the 16S experiment. C.N., G.B., and L.Z. provided critical comments and suggestions. L.Z. provided human samples. J.H. and S.Z. wrote the manuscript. S.Z. supervised the project.

DECLARATION OF INTERESTS

S.Z. is a co-founder of Ibiome, which studies microbial regulation of immune responses.

Received: July 31, 2023
Revised: November 24, 2023
Accepted: February 1, 2024
Published: February 26, 2024

REFERENCES

1. Writing Group for the TRIGR Study Group; Knip, M., Åkerblom, H.K., Al Taji, E., Becker, D., Bruining, J., Castano, L., Danne, T., de Beaufort, C., Dosch, H.M., et al. (2018). Effect of Hydrolyzed Infant Formula vs Conventional Formula on Risk of Type 1 Diabetes: The TRIGR Randomized Clinical Trial. JAMA *319*, 38–48. https://doi.org/10.1001/jama.2017.19826.
2. Verduci, E., Salvatore, S., Bresesti, I., Di Profio, E., Pendezza, E., Bosetti, A., Agosti, M., Zuccotti, G.V., and D'Auria, E. (2021). Semi-Elemental and Elemental Formulas for Enteral Nutrition in Infants and Children with Medical Complexity-Thinking about Cow's Milk Allergy and Beyond. Nutrients *13*, 4230. https://doi.org/10.3390/nu13124230.
3. Munblit, D., Perkin, M.R., Palmer, D.J., Allen, K.J., and Boyle, R.J. (2020). Assessment of Evidence About Common Infant Symptoms and Cow's Milk Allergy. JAMA Pediatr. *174*, 599–608. https://doi.org/10.1001/jamapediatrics.2020.0153.
4. Mullen, A. (2022). Cow's milk allergy guidelines for infants. Nat. Food *3*, 5. https://doi.org/10.1038/s43016-021-00456-w (2022.
5. Fleischer, D.M., Venter, C., and Vandenplas, Y. (2016). Hydrolyzed Formula for Every Infant? Nestle Nutr. Inst. Workshop Ser. *86*, 51–65. https://doi.org/10.1159/000442956.
6. Hickman, N., Morgan, S., Crawley, H., and Kerac, M. (2021). Advertising of Human Milk Substitutes in United Kingdom Healthcare Professional Publications: An Observational Study. J. Hum. Lactation *37*, 674–682. https://doi.org/10.1177/08903344211018161.
7. Miqdady, M., AlMutaeri, S., Alsawi, N., Goronfolah, L., Tzivinikos, C., Al Hameli, H., Cremonesini, D., Al-Enezi, M., Hussain, A., Al Damerdash, Z., and Al-Biltagi, M. (2023). Budget Impact of Early Introduction of Amino Acid Formula in Managing Infants with Cow Milk Protein Allergy: Arabian Gulf Countries' Experience. J. Asthma Allergy *16*, 73–82. https://doi.org/10.2147/jaa.S390352.
8. Sheikh, C., and Erickson, P.R. (1996). Evaluation of plaque pH changes following oral rinse with eight infant formulas. Pediatr. Dent. *18*, 200–204.
9. Vandenplas, Y., Żołnowska, M., Berni Canani, R., Ludman, S., Tengelyi, Z., Moreno-Álvarez, A., Goh, A.E.N., Gosoniu, M.L., Kirwan, B.A., Tadi, M., et al. (2022). Effects of an Extensively Hydrolyzed Formula Supplemented with Two Human Milk Oligosaccharides on Growth, Tolerability, Safety and Infection Risk in Infants with Cow's Milk Protein Allergy: A Randomized, Multi-Center Trial. Nutrients *14*, 530. https://doi.org/10.3390/nu14030530.
10. D'Auria, E., et al. (2021). Hydrolysed Formulas in the Management of Cow's Milk Allergy: New Insights, Pitfalls and Tips. Nutrients *13*. https://doi.org/10.3390/nu13082762.
11. Lee, B., Wang, Y., Carlson, S.A., Greenlund, K.J., Lu, H., Liu, Y., Croft, J.B., Eke, P.I., Town, M., and Thomas, C.W. (2023). National, State-Level, and County-Level Prevalence Estimates of Adults Aged ≥18 Years Self-Reporting a Lifetime Diagnosis of Depression - United States, 2020. MMWR Morb. Mortal. Wkly. Rep. *72*, 644–650. https://doi.org/10.15585/mmwr.mm7224a1.
12. Akbaraly, T.N., Brunner, E.J., Ferrie, J.E., Marmot, M.G., Kivimaki, M., and Singh-Manoux, A. (2009). Dietary pattern and depressive symptoms in middle age. Br. J. Psychiatry *195*, 408–413. https://doi.org/10.1192/bjp.bp.108.058925.
13. Bayes, J., Schloss, J., and Sibbritt, D. (2022). The effect of a Mediterranean diet on the symptoms of depression in young males (the "AMMEND: A Mediterranean Diet in MEN with Depression" study): a randomized controlled trial. Am. J. Clin. Nutr. *116*, 572–580. https://doi.org/10.1093/ajcn/nqac106.
14. Makki, K., Deehan, E.C., Walter, J., and Bäckhed, F. (2018). The Impact of Dietary Fiber on Gut Microbiota in Host Health and Disease. Cell Host Microbe *23*, 705–715. https://doi.org/10.1016/j.chom.2018.05.012.
15. Agus, A., Planchais, J., and Sokol, H. (2018). Gut Microbiota Regulation of Tryptophan Metabolism in Health and Disease. Cell Host Microbe *23*, 716–724. https://doi.org/10.1016/j.chom.2018.05.003.
16. Cryan, J.F., and Dinan, T.G. (2012). Mind-altering microorganisms: the impact of the gut microbiota on brain and behaviour. Nat. Rev. Neurosci. *13*, 701–712. https://doi.org/10.1038/nrn3346.
17. Mayneris-Perxachs, J., Castells-Nobau, A., Arnoriaga-Rodríguez, M., Martin, M., de la Vega-Correa, L., Zapata, C., Burokas, A., Blasco, G., Coll, C., Escrichs, A., et al. (2022). Microbiota alterations in proline metabolism impact depression. Cell Metabol. *34*, 681–701.e10. https://doi.org/10.1016/j.cmet.2022.04.001.
18. He, K., Wan, T., Wang, D., Hu, J., Zhou, T., Tao, W., Wei, Z., Lu, Q., Zhou, R., Tian, Z., et al. (2023). Gasdermin D licenses MHCII induction to maintain food tolerance in small intestine. Cell *186*, 3033–3048.e20. https://doi.org/10.1016/j.cell.2023.05.027.
19. Kok, C.R., Brabec, B., Chichlowski, M., Harris, C.L., Moore, N., Wampler, J.L., Vanderhoof, J., Rose, D., and Hutkins, R. (2020). Stool microbiome, pH and short/branched chain fatty acids in infants receiving extensively hydrolyzed formula, amino acid formula, or human milk through two months of age. BMC Microbiol. *20*, 337. https://doi.org/10.1186/s12866-020-01991-5.
20. He, K., Wan, T., Wang, D., Hu, J., Zhou, T., Tao, W., Wei, Z., Lu, Q., Zhou, R., Tian, Z., et al. (2023). Gasdermin D licenses MHCII induction to maintain food tolerance in small intestine. Cell *186*, 3033–3048.e20. https://doi.org/10.1016/j.cell.2023.05.027.
21. Schiffman, S.S., Sennewald, K., and Gagnon, J. (1981). Comparison of taste qualities and thresholds of D- and L-amino acids. Physiol. Behav. *27*, 51–59. https://doi.org/10.1016/0031-9384(81)90298-5.
22. Herman, J.P., McKlveen, J.M., Ghosal, S., Kopp, B., Wulsin, A., Makinson, R., Scheimann, J., and Myers, B. (2016). Regulation of the Hypothalamic-Pituitary-Adrenocortical Stress Response. Compr. Physiol. *6*, 603–621. https://doi.org/10.1002/cphy.c150015.
23. Holsboer, F. (2000). The corticosteroid receptor hypothesis of depression. Neuropsychopharmacology *23*, 477–501. https://doi.org/10.1016/s0893-133x(00)00159-7.
24. Robinette, M.L., and Colonna, M. (2014). GI motility: microbiota and macrophages join forces. Cell *158*, 239–240. https://doi.org/10.1016/j.cell.2014.06.040.
25. de Medeiros, M.A., Carlos Reis, L., and Eugênio Mello, L. (2005). Stress-induced c-Fos expression is differentially modulated by dexamethasone, diazepam and imipramine. Neuropsychopharmacology *30*, 1246–1256. https://doi.org/10.1038/sj.npp.1300694.
26. Beck, C.H., and Fibiger, H.C. (1995). Conditioned fear-induced changes in behavior and in the expression of the immediate early gene c-fos: with and without diazepam pretreatment. J. Neurosci. *15*, 709–720. https://doi.org/10.1523/jneurosci.15-01-00709.1995.
27. Clemmensen, C., Müller, T.D., Woods, S.C., Berthoud, H.R., Seeley, R.J., and Tschöp, M.H. (2017). Gut-Brain Cross-Talk in Metabolic Control. Cell *168*, 758–774. https://doi.org/10.1016/j.cell.2017.01.025.
28. de Oliveira, J., Engel, D.F., de Paula, G.C., Dos Santos, D.B., Lopes, J.B., Farina, M., Moreira, E.L.G., and de Bem, A.F. (2020). High Cholesterol Diet Exacerbates Blood-Brain Barrier Disruption in LDLr-/- Mice: Impact on Cognitive Function. J. Alzheimers Dis. *78*, 97–115. https://doi.org/10.3233/jad-200541.
29. Fan, K.Q., Li, Y.Y., Wang, H.L., Mao, X.T., Guo, J.X., Wang, F., Huang, L.J., Li, Y.N., Ma, X.Y., Gao, Z.J., et al. (2019). Stress-Induced Metabolic Disorder in Peripheral CD4(+) T Cells Leads to Anxiety-like Behavior. Cell *179*, 864–879.e19. https://doi.org/10.1016/j.cell.2019.10.001.

30. Lamichhane, S., Siljander, H., Salonen, M., Ruohtula, T., Virtanen, S.M., Ilonen, J., Hyötyläinen, T., Knip, M., and Orešič, M. (2022). Impact of Extensively Hydrolyzed Infant Formula on Circulating Lipids During Early Life. Front. Nutr. *9*, 859627. https://doi.org/10.3389/fnut.2022.859627.

31. Knudsen, J.K., Michaelsen, T.Y., Bundgaard-Nielsen, C., Nielsen, R.E., Hjerrild, S., Leutscher, P., Wegener, G., and Sørensen, S. (2021). Faecal microbiota transplantation from patients with depression or healthy individuals into rats modulates mood-related behaviour. Sci. Rep. *11*, 21869. https://doi.org/10.1038/s41598-021-01248-9 (2021.

32. Li, N., Wang, Q., Wang, Y., Sun, A., Lin, Y., Jin, Y., and Li, X. (2019). Fecal microbiota transplantation from chronic unpredictable mild stress mice donors affects anxiety-like and depression-like behavior in recipient mice via the gut microbiota-inflammation-brain axis. Stress *22*, 592–602. https://doi.org/10.1080/10253890.2019.1617267.

33. O'Neil, A., Quirk, S.E., Housden, S., Brennan, S.L., Williams, L.J., Pasco, J.A., Berk, M., and Jacka, F.N. (2014). Relationship between diet and mental health in children and adolescents: a systematic review. Am. J. Publ. Health *104*, e31–e42. https://doi.org/10.2105/ajph.2014.302110.

34. Parletta, N., Zarnowiecki, D., Cho, J., Wilson, A., Bogomolova, S., Villani, A., Itsiopoulos, C., Niyonsenga, T., Blunden, S., Meyer, B., et al. (2019). A Mediterranean-style dietary intervention supplemented with fish oil improves diet quality and mental health in people with depression: A randomized controlled trial (HELFIMED). Nutr. Neurosci. *22*, 474–487. https://doi.org/10.1080/1028415x.2017.1411320.

35. Quirk, S.E., Williams, L.J., O'Neil, A., Pasco, J.A., Jacka, F.N., Housden, S., Berk, M., and Brennan, S.L. (2013). The association between diet quality, dietary patterns and depression in adults: a systematic review. BMC Psychiatr. *13*, 175. https://doi.org/10.1186/1471-244x-13-175.

36. O'Mahony, S.M., Clarke, G., Borre, Y.E., Dinan, T.G., and Cryan, J.F. (2015). tryptophan metabolism and the brain-gut-microbiome axis. Behav. Brain Res. *277*, 32–48. https://doi.org/10.1016/j.bbr.2014.07.027.

37. Olm, M.R., Dahan, D., Carter, M.M., Merrill, B.D., Yu, F.B., Jain, S., Meng, X., Tripathi, S., Wastyk, H., Neff, N., et al. (2022). Robust variation in infant gut microbiome assembly across a spectrum of lifestyles. Science *376*, 1220–1223. https://doi.org/10.1126/science.abj2972.

38. Xu, G., Snetselaar, L.G., Jing, J., Liu, B., Strathearn, L., and Bao, W. (2018). Association of Food Allergy and Other Allergic Conditions With Autism Spectrum Disorder in Children. JAMA Netw. Open *1*, e180279. https://doi.org/10.1001/jamanetworkopen.2018.0279.

39. Nemet, S., Asher, I., Yoles, I., Baevsky, T., and Sthoeger, Z. (2022). Early childhood allergy linked with development of attention deficit hyperactivity disorder and autism spectrum disorder. Pediatr. Allergy Immunol. *33*. https://doi.org/10.1111/pai.13819.

40. Suez, J., Zmora, N., Zilberman-Schapira, G., Mor, U., Dori-Bachash, M., Bashiardes, S., Zur, M., Regev-Lehavi, D., Ben-Zeev Brik, R., Federici, S., et al. (2018). Post-Antibiotic Gut Mucosal Microbiome Reconstitution Is Impaired by Probiotics and Improved by Autologous FMT. Cell *174*, 1406–1423.e16. https://doi.org/10.1016/j.cell.2018.08.047.

41. Wang, H., Zhu, Q., Ding, L., Shen, Y., Yang, C.Y., Xu, F., Shu, C., Guo, Y., Xiong, Z., Shan, Q., et al. (2019). Scalable volumetric imaging for ultrahigh-speed brain mapping at synaptic resolution. Natl. Sci. Rev. *6*, 982–992. https://doi.org/10.1093/nsr/nwz053.

42. Porsolt, R.D., Anton, G., Blavet, N., and Jalfre, M. (1978). Behavioural despair in rats: a new model sensitive to antidepressant treatments. Eur. J. Pharmacol. *47*, 379–391. https://doi.org/10.1016/0014-2999(78)90118-8.

43. Cryan, J.F., Mombereau, C., and Vassout, A. (2005). The tail suspension test as a model for assessing antidepressant activity: review of pharmacological and genetic studies in mice. Neurosci. Biobehav. Rev. *29*, 571–625. https://doi.org/10.1016/j.neubiorev.2005.03.009.

44. An, K., Zhao, H., Miao, Y., Xu, Q., Li, Y.F., Ma, Y.Q., Shi, Y.M., Shen, J.W., Meng, J.J., Yao, Y.G., et al. (2020). A circadian rhythm-gated subcortical pathway for nighttime-light-induced depressive-like behaviors in mice. Nat. Neurosci. *23*, 869–880. https://doi.org/10.1038/s41593-020-0640-8.

45. Sakata, K., Jin, L., and Jha, S. (2010). Lack of promoter IV-driven BDNF transcription results in depression-like behavior. Gene Brain Behav. *9*, 712–721. https://doi.org/10.1111/j.1601-183X.2010.00605.x.

46. Mao, X., Ou, M.T., Karuppagounder, S.S., Kam, T.I., Yin, X., Xiong, Y., Ge, P., Umanah, G.E., Brahmachari, S., Shin, J.H., et al. (2016). Pathological α-synuclein transmission initiated by binding lymphocyte-activation gene 3. Science *353*, aah3374. https://doi.org/10.1126/science.aah3374.

47. Kim, S., et al. (2019). Transneuronal Propagation of Pathologic α-Synuclein from the Gut to the Brain Models Parkinson's Disease. Neuron *103*, 627–641.e627. https://doi.org/10.1016/j.neuron.2019.05.035.

48. Ekstrand, E., Lexell, J., and Brogårdh, C. (2016). Grip strength is a representative measure of muscle weakness in the upper extremity after stroke. Top. Stroke Rehabil. *23*, 400–405. https://doi.org/10.1080/10749357.2016.1168591.

49. Kwon, S.H., Lee, H.K., Kim, J.A., Hong, S.I., Kim, H.C., Jo, T.H., Park, Y.I., Lee, C.K., Kim, Y.B., Lee, S.Y., and Jang, C.G. (2010). Neuroprotective effects of chlorogenic acid on scopolamine-induced amnesia via anti-acetylcholinesterase and anti-oxidative activities in mice. Eur. J. Pharmacol. *649*, 210–217. https://doi.org/10.1016/j.ejphar.2010.09.001.

50. Bevins, R.A., and Besheer, J. (2006). Object recognition in rats and mice: a one-trial non-matching-to-sample learning task to study 'recognition memory. Nat. Protoc. *1*, 1306–1311. https://doi.org/10.1038/nprot.2006.205.

51. Vorhees, C.V., and Williams, M.T. (2006). Morris water maze: procedures for assessing spatial and related forms of learning and memory. Nat. Protoc. *1*, 848–858. https://doi.org/10.1038/nprot.2006.116.

52. Kalueff, A.V., Aldridge, J.W., LaPorte, J.L., Murphy, D.L., and Tuohimaa, P. (2007). Analyzing grooming microstructure in neurobehavioral experiments. Nat. Protoc. *2*, 2538–2544. https://doi.org/10.1038/nprot.2007.367.

53. Shin Yim, Y., Park, A., Berrios, J., Lafourcade, M., Pascual, L.M., Soares, N., Yeon Kim, J., Kim, S., Kim, H., Waisman, A., et al. (2017). Reversing behavioural abnormalities in mice exposed to maternal inflammation. Nature *549*, 482–487. https://doi.org/10.1038/nature23909.

54. Golden, S.A., Covington, H.E., 3rd, Berton, O., and Russo, S.J. (2011). A standardized protocol for repeated social defeat stress in mice. Nat. Protoc. *6*, 1183–1191. https://doi.org/10.1038/nprot.2011.361.

55. Baudry, C., Reichardt, F., Marchix, J., Bado, A., Schemann, M., des Varannes, S.B., Neunlist, M., and Moriez, R. (2012). Diet-induced obesity has neuroprotective effects in murine gastric enteric nervous system: involvement of leptin and glial cell line-derived neurotrophic factor. J. Physiol. *590*, 533–544. https://doi.org/10.1113/jphysiol.2011.219717.

56. Osinski, M.A., Bass, P., and Gaumnitz, E.A. (1999). Peripheral and central actions of orphanin FQ (nociceptin) on murine colon. Am. J. Physiol. *276*, G125–G131. https://doi.org/10.1152/ajpgi.1999.276.1.G125.

57. Tasselli, M., Chaumette, T., Paillusson, S., Monnet, Y., Lafoux, A., Huchet-Cadiou, C., Aubert, P., Hunot, S., Derkinderen, P., and Neunlist, M. (2013). Effects of oral administration of rotenone on gastrointestinal functions in mice. Neuro Gastroenterol. Motil. *25*, e183–e193. https://doi.org/10.1111/nmo.12070.

58. Choi, Y.J., Kim, J.E., Lee, S.J., Gong, J.E., Son, H.J., Hong, J.T., and Hwang, D.Y. (2021). Dysbiosis of Fecal Microbiota From Complement 3 Knockout Mice With Constipation Phenotypes Contributes to Development of Defecation Delay. Front. Physiol. *12*, 650789. https://doi.org/10.3389/fphys.2021.650789.

59. Xie, Z., Zhang, X., Zhao, M., Huo, L., Huang, M., Li, D., Zhang, S., Cheng, X., Gu, H., Zhang, C., et al. (2022). The gut-to-brain axis for toxin-induced defensive responses. Cell *185*, 4298–4316.e21. https://doi.org/10.1016/j.cell.2022.10.001.

60. Ma, H., Hu, T., Tao, W., Tong, J., Han, Z., Herndler-Brandstetter, D., Wei, Z., Liu, R., Zhou, T., Liu, Q., et al. (2023). A lncRNA from an inflammatory bowel disease risk locus maintains intestinal host-commensal homeostasis. Cell Res. *33*, 372–388. https://doi.org/10.1038/s41422-023-00790-7 (2023.

STAR★METHODS

KEY RESOURCES TABLE

REAGENT or RESOURCE	SOURCE	IDENTIFIER
Antibodies		
Anti-rabbit cFos	Cell signing technology	Cat#2250S; RRID: AB_2313773
Anti-Rabbit IgG (H + L), CF™ 488A antibody	Sigma	Cat#A-11034; RRID: AB_2313773
Chemicals, peptides, and recombinant proteins		
Corticosterone	MedChemExpress	Cat#HY-B1618
Carmine Dye	Sigma-Aldrich	Cat#1390-65-4
Sodium carboxymethyl cellulose	Sigma-Aldrich	Cat#9004-32-4
Evans blue Dye	Sigma-Aldrich	Cat#314-13-6
Vancomycin	Sangon	Cat#1404-93-9
Neomycin	Sangon	Cat#1405-10-3
Ampicillin	Sangon	Cat#69-52-3
Metronidazole	Sangon	Cat#443-48-1
DAPI	Biolegend	Cat#422801
Acetonitrile, for HPLC	Sangon	Cat#75-05-8
Methyl alcohol, for HPLC	Sangon	Cat#67-56-1
Acrylamide	Sangon	Cat#A100341
Bis-acrylamide	Sangon	Cat#A100172
VA-044	Aladdin	Cat#A151317
Boric acid	Sangon	Cat#A100588
Iohexol	Sangon	Cat#A611182
Triton X-100	Sangon	Cat#A600198
Donkey serum	Sigma-Aldrich	Cat#ab7475
Disodium hydrogenphosphate, anhydrous	Sangon	Cat#A610404
Sodium dihydngen phoshate anhydrous	Sangon	Cat#A600878
Critical commercial assays		
GeneJET PCR Purification Kit	Thermo Fisher Scientific	Cat#K0702
Deposited data		
16s RNA sequencing	NCBI BioProject ID	PRJNA1066063 PRJNA1068313 PRJNA1068747
Experimental models: Organisms/strains		
C57BL/6JGpt	GemPharmatech	Strain NO. N000013
Rag-1$^{-/-}$ mice	GemPharmatech	Strain NO. T004753
Oligonucleotides		
16s RNA 515F Forward barcode primer, AATGATACGGC GACCACCGAGATCTACACGCTXXXXXXXXXXXXXTATGGT AATTGTGTGYCAGCMGCCGCGGTAA	This paper	N/A
16s RNA 806R reverse primer, CAAGCAG AAGACGGCATACGAGATAGTCAGCCAGC CGGACTACNVGGGTWTCTAAT.	This paper	N/A
Read 1, TATGGTAATT GT GTGYCAGCMGCCGCGGTAA	This paper	N/A
Read 2, AGTCAGCCAG CC GGACTACNVGGGTWTCTAAT	This paper	N/A
Index: AATGATACGGCGACCACCGAGATCTACACGCT	This paper	N/A
Software and algorithms		
Prism version 9	Graphpad	https://www.graphpad.com/
CaseViewer 2.4	3DHISTECH	https://www.3dhistech.com/solutions/caseviewer/
Ethovision XT 12	Noldus	https://www.noldus.com/ethovision-xt

(*Continued on next page*)

Continued

REAGENT or RESOURCE	SOURCE	IDENTIFIER
Imaris 9.21	Bitplane	https://imaris.oxinst.com/
Qiime2 v2023.2	QIIME 2	https://qiime2.org/
ImageJ	NIH	https://imagej.nih.gov/ij/
Peak View 2.2	SCIEX	https://sciex.com/products/software/peakview-software
TissueFAXS PLUS	Gmbh	https://tissuegnostics.com/products/scanning-and-viewing-software/tissuefaxs-imaging-software

RESOURCE AVAILABILITY

Lead contact

Further information and requests for resources and reagents should be directed to and will be fulfilled by the lead contact, Shu Zhu (zhushu@ustc.edu.cn).

Materials availability

All materials generated in this study are available from the lead contact upon request.

Data and code availability

- The data supporting the findings of this study are available within the article and its supplemental information. The 16s RNA sequencing datasets generated in this study can be found in the NCBI SRA database (http://www.ncbi.nlm.nih.gov/sra/) using the access number PRJNA1066063, PRJNA1068313, PRJNA1068747.
- This paper does not report original code.
- Any additional information required to reanalyze the data reported in this work paper is available from the lead contact upon request.

EXPERIMENTAL MODEL AND STUDY PARTICIPANT DETAILS

Mice

The AAD-feeding experiments used mice were C57BL/6J (B6) strain and purchased from Gempharmatech, China. *Rag1*$^{-/-}$ mice were purchased from GemPharmatech, China. All experiments used mice were 3 days–old to 10 weeks-old, age- and sex-matched male mice. All mice were maintained under specific pathogen-free (SPF) conditions and kept at a strict 24 h light-dark cycle, with lights on from 8 a.m. to 8 p.m. in the animal facility of the University of Science and Technology of China. All animal experiments were approved by the Ethics Committee of University of Science and Technology of China (USTCACUC23120123039).

Human participants

Human feces from CMF- (n = 28) and AAF-fed (n = 32) infants were obtained from the First Affiliated Hospital of USTC, University of Science and Technology of China. All human experiments were approved by the Ethics Committee of the First Affiliated Hospital of USTC, University of Science and Technology of China (2023-RE-208).

METHOD DETAILS

Amino acid diet

AAD was customized from Medicience (Jiangsu, CN), as previously reported.[20] The AAD ingredient was listed as follows (g/kg): L-Alanine 4.5; L-Arginine, 6.3; L-Aspartic Acid 11.3; L-Cystine 3.7; L-Glutamic Acid 36.2; Glycine 3.1; L-Histidine, 4.5; L-Isoleucine 8.4; L-Leucine 15.3; L-Lysine-HCl 16.1; L-Methionine 4.5; L-Phenylalanine 8.7; L-Proline 20.4; L-Serine 9.4; L-Threonine 6.6; L-Tryptophan 2.1; L-Tyrosine 9.2; L-Valine 9.9; Sucrose 100; Cornstarch 399.886; Dyetrose 145; Soybean Oil 70; tBHQ 0.014; Cellulose 50; Salt Mix 35; Sodium Bicarbonate 7.4; Vitamin Mix 10; Choline Bitartrate 2.5 (Table S1). All diets were irradiated and vacuum-packed. The feeding method of AAD to mouse starts at 3 days of age and continued for 4 weeks. All mice were allowed free access to water.

AAD mouse model

Neonatal littermates C57BL/B6J male mice were fed with AAD from the age of 3 days–4 weeks and switched to NCD for 2 weeks. At the age of 6 weeks, the mice were taken behavior tests and GI motility tests. Upon the termination of experiments, mice were sacrificed by CO_2 asphyxiation.

ABX treatment

C57BL/6 wild-type mice were supplied with a mixture of antibiotics (ampicillin 1 mg/mL, neomycin 1 mg/mL, metronidazole 1 mg/mL, and vancomycin 0.5 mg/mL) (key resources table) in drinking water for one week. Fresh feces samples were collected for the measurement of fecal bacteria load.

Fecal microbiota transplantation

Fecal microbiota transplantation (FMT) was performed according to a reported protocol.[40] Briefly, fecal pellets from donor mice (NCD- and AAD-fed mice) were collected in sterile conditions. The pellets from each donor mouse were separately resuspended in sterile PBS under anaerobic conditions (75% N_2, 20% CO_2, 5% H_2) with vigorous mixing for 3 min, and allowed to settle by gravity for 2 min. Samples were immediately transferred to the animal facility and the supernatant was administered to recipient C57BL/6 wild-type mice by oral gavage.

16S-microbiota sequencing

Fecal samples were taken from mice at the indicated time points and stored at −80°C until 16S rRNA analysis. DNA was extracted from fecal pellets with GeneJET PCR Purification Kit (key resources table) according to the manufacturer's instructions, and normalized to 10 ng/μL. 16S rRNA amplicons were generated using the primer 515F/806R recommended by the Earth Microbiome Project 2. The primer used are in the key resources table. MiSeq (Illumina) fastq files were analyzed using Qiime2 (v.2023.2.0). Using the Illumina bcl2fastq (v.2.20) and the barcode mapping file, the reads were demultiplexed and assigned to their corresponding sample. Denoising and amplicon sequencing variants (ASV) tables were constructed using DADA2 plugin via command dada2-denoise-paired. Samples that did not reach the established sequencing depths (512 reads for mice sample, 2283 for human sample) were excluded from further diversity analysis. Diversity analysis results were generated using the diversity-core-metrics-phylogenetic plugin. ASVs were assigned with taxonomic annotations by applying the feature-classifier plugin (classify-sklearn) to our representative sequences and using a naive Bayes taxonomic classifier downloaded from Qiime's data-resources page. Linear discriminant analysis Effect Size (LEfSe) was used to determine the bacterial taxa with significant differences in abundance between different groups.

Immunofluorescence staining

The colon and brain tissues were isolated, fixed in 4% PFA overnight, washed with PBS, cryo-protected in 30% sucrose solution overnight, then processed through OCT embedding, and finally colon tissues were cut into 10-μm-thin sections, brain tissues were cut into 50-μm-thin sections. The sections were permeated and blocked in blocking solution (5% donkey serum (w/v), 0.3% Triton X-100 in PBS) (key resources table) for 1 h. The primary antibodies for immunofluorescence were Rabbit-*anti*-cFos (9F6) antibody (key resources table). Antibody were incubated in 1% diluted blocking buffer overnight at dilutions of 1: 1000 at 4°C; the sections were washed 3 times with PBS and incubated with a secondary antibody (Anti-Rabbit IgG (H + L), CF 488A antibody) (key resources table) at dilutions 1: 200 in 1% blocking buffer for 1 h at room temperature. Subsequently, sections were washed with PBS three times, counterstained with DAPI (1 μg/mL) (key resources table) in PBS for 10 min, then visualized using TissueFAXS PLUS (TissueGnostics Gmbh) imaging system and imaris v9.8 (bitplane, Oxford Instruments). ImageJ software was used to detect the protein gray value.

cFos staining

cFos staining were performed according to protocols.[41] Fixed brains were cut into 300-μm-thick slices using a vibroslicer (Compresstome VF-300, Precisionary Instruments). The brain slices were then transferred into 12-well plates and washed 4 times with PBS for 1 h each time. After that, the slices were polymerized in Hydrogel Monomer Solution (HMS) (4% Acrylamide (w/v), 0.1% Bis-acrylamide (w/v), 0.25% VA-044 (w/v) in 50mL 4% PFA, 3mL per mouse) (key resources table) for post-fixation and then were polymerized for 4 h at 37°C in the absence of air. After polymerization, the gel around the slices were peel off. Then transfer the slices into Clean Buffer (CB) (4% SDS (w/v), 1.2% Borate (w/v) in ddH_2O) (key resources table) pH 8.5 and gently shake them in 4°C for 24h. After clearing, the slices were washed 4 times with PBS for 1 h each time. Cleared slices were loaded into 12-well plates, permeated and blocked in blocking solution (3% donkey serum (w/v), 0.3% Triton X-100 in PBS) (key resources table) for 1 h and then incubated with primary antibody (Rabbit-*anti*-cFos (9F6) antibody, dilution 1:1000) (key resources table) in blocking solution overnight in 4°C, followed by washing in 0.3% PBST three times for 1 h each. The slices were then incubated in secondary antibody (Anti-Rabbit IgG (H + L), CF 488A antibody, dilution 1:200) (key resources table) at room temperature for 5 h, followed by washing in 0.3% PBST for three times. Finally, the slices of an entire mouse brain were mounted onto a customized slide by the order of slicing with the same surface upward. Then the slide was transferred into an imaging chamber which is filled with Refractive Index Matching Solution, (RIMS) (133.3% iohexol (w/v) in 0.02M PB) (key resources table) pH 7.4. Whole-brain image reconstruction was used the VISoR system and performed as described previously.[41]

Assessment of corticosterone levels

Serum were collected 100 μL on the day of sacrifice and homogenized with 400 μL prechilled methanol/acetonitrile (1:1, v/v) (key resources table), thoroughly mixed 5 min by vortexing. The mixture underwent ultrasonication for 10 min. Liquid nitrogen was then used to quench the sample for 1 min, followed by melting at room temperature. This ultrasonication and quenching process was repeated three times. The resulting mixture was incubated at −20°C for 4-6 h to facilitate protein precipitation. Afterward, centrifugation was performed at 13,000 rpm for 15 min at 4°C. The resulting supernatant was then transferred to LC vials.

The corticosterone levels were measured by LC-MS/MS (LCMS-8050, SHIMADZU), separation was achieved using an Waters ACQUITY UPLC C18 (100 mm × 2.1 mm, 1.7 μm). The mobile phases consisted of solvent A (0.1% acetic acid amine in water) and solvent B (methyl alcohol) (key resources table) at a flow rate 0.3 mL/min. The injection volume was 1 μL and the column temperature was set at 35°C. The gradient flow started at 10% B for 1 min, linearly increased to 60% B over the next 4 min, further linearly increased to 95% B over the subsequent 9 min. It was then linearly decreased to 10% B within the next 0.5 min and maintained at this composition for an additional 2 min. Peaks were identified based on the retention time of the standards and confirmed by comparison of the wavelength scan spectra (set between 210 nm and 400 nm). The analysis was performed in positive-ion mode, and data processing was done using Peak View 2.2 software based on m/z values and sample retention time.

Behavior tests

To evaluate AAD-fed induced behavioral deficits, AAD and NCD-fed mice were assessed by the open field test, tail suspension test, forced swimming test and sucrose preference for depressive-like test, pole test, rotarod test, and grip strength test for motor deficits, and spontaneous alternation behavior Y-maze test, novel object recognition test, step-through passive avoidance test, Morris water maze test, grooming test, marble burying test, social interaction test, for cognition deficits. The experimenter was blinded to treatment group for all behavioral studies. All tests were performed and recorded between 10:00–16:00 in the lights-on cycle. All animals were allowed to the experimental room for 1 h before the training.

Forced swim test

Mice were placed in a glass beaker (30 cm tall, 20 cm diameter) containing 15cm high water at 24 ± 1 °C. Mice were allowed to swim for 6 min. Prepared video camera in front of the beakers so that perceived every beaker in a way that allow the clear observation of the animals' behavior later on while viewing the footage. Immobility was quantified the last 4 min by two blinded, trained experimenters. Code the duration of time spent as ''Immobile'' if the mouse is floating with the absence of any movement except for those necessary for keeping the nose above water. Code the duration of time spent as ''Swimming'' if movement of forelimbs or hind limbs in a paddling fashion is observed. Data were expressed as immobility time (min) in different groups.[42]

Tail suspension test

Mice were suspended by their tail from a lever in a 30 × 15 × 15cm blue-painted enclosure. Movements were recorded for 6 min in a quiet environment. The behavior of the animal was recorded by a side camera for 6 min, and the duration of immobility was quantified the last 4 min by two blinded, trained experimenters. The first 2 min were excluded due to high stress. Data were expressed as immobility time (min) in different groups.[43]

Sucrose preference

Sucrose preference test was performed as previously reported,[44] mice were single housed to acclimatize to two bottles of water for 24 h, then subjected to water deprivation for 24 h, followed by the 24h testing period (starting from 14:00) during which the mice were provided with one bottle of 1% sucrose (w/v) and one bottle of water. The position of the two bottles was switched at 2 h and 6 h. The percentage of sucrose preference was calculated as the following calculation method: % Sucrose preference = the consumption of 1% sucrose/the total liquid consumed (water and sucrose) x 100.

Open field test (OFT)

The open field consisted of a rectangular plastic box (50 cm × 50 cm x 50 cm) divided into 36 (6 x 6) identical sectors (6.6 cm × 6.6 cm). The field was subdivided into peripheral and central sectors, where the central sector included 4 central squares (2 x 2) and the peripheral sector was the remaining squares.[45] The mouse was placed into the center of an open field and allowed to explore for 6 min. The apparatus was thoroughly cleaned with diluted 75% ethanol between each trial. A video tracking system (Ethovision XT software) was used to analyze the distance traveled as a measure of locomotor activity. The time spent in and entries into the center were measured as an anxiolytic indicator.[45]

Pole test

The pole was composed of a 75 cm of metal rod with a diameter of 9 mm. It was wrapped with bandage gauze, putting in a clean cage with bedding.[46] Mice were placed on the top of the pole (7.5 cm from the top of the pole) facing the head-up. Total time taken to reach the base of the pole was recorded. Before the actual test, mice were trained for two consecutive days. Each training session consisted of three test trials. On the test day, mice were evaluated in three sessions and total time was recorded. The maximum cut off time to stop the test and recording was 60 s. Results for the total time (sec) were recorded.

Hanging test

The mice were placed in the center of a 30 × 30 cm^2 screen with a 1-cm-wide mesh. The screen was inverted head-over-tail and placed on supports 40 cm above an open, clean cage with bedding. Mice were timed until they released their grip or remained for 60s. Data were expressed as hanging time (min) in different groups.

Freezing test

Mice were individually placed in a chamber with a grid floor connected to a shock generator (MED-SYST-VFC, MED). Two minutes after being placed in the chamber, the mice were exposed to a 3 s foot shock (0.6 mA) for 5 times during 120 s randomly. SMART3.0 tracking system record the freezing time between different groups.

Rotarod test

For the rotarod test, the mice were trained 3 days before test. On the test day, mice were placed on an accelerating rotarod cylinder (LE8505, Panlab), and the latency time of the animals was measured. The speed was slowly increased from 4 to 40 rpm within 5 min. A trial ended if the animal fell off the rungs or gripped the device and spun around for 2 consecutive revolutions without attempting to walk on the rungs. Motor test data are presented as mean of latency time (min) on the rotarod.[47]

Grip strength test

Neuromuscular strength testing was performed using a grip strength test machine as previously described.[48] Performance of the mice was assessed three times. To assess grip strength, mice were allowed to grasp a metal grid either by their fore limbs or both fore and hind limbs. The tail was gently pulled and the maximum holding force recorded by the force transducer (BIO-GS3, Bioseb) when the mice released their grasp on the grid. The peak holding strength was digitally recorded and displayed as force in grams. Grip strength was scored as grams (g).

Spontaneous alternation behavior Y-maze test

A spontaneous alternation behavior Y-maze test was performed as described.[49] The Y-maze is a horizontal maze with three equal angles between all arms, which were 40 cm long and 10 cm wide with 15 cm high walls. The maze floor and walls were constructed using opaque polyvinyl plastic. Mice were initially placed within one arm, and the sequence and number of arm entries were recorded manually for each mouse over an 8-min period. A spontaneous alternation was defined in which the mice entered all three arms, i.e., ABC, CAB, or BCA but not ABB, was recorded as an alternation to precision short-term memory. The alternation score (%) for each mouse was calculated as the ratio of the actual number of alternations to the possible number (defined as the total number of arm entries minus two) multiplied by 100 as shown by the following equation: % Alternative behavior = [(Number of alternations)/(Total arm entries – 2)] x100. The number of arm entries per trial was used as an indicator of locomotor activity. The Y-maze arms were cleaned with diluted 75% ethanol between tests to eliminate odors and residues.

Novel object recognition test (NORT)

The NORT was performed according to the conventional protocol.[50] NORT were carried out in a white open field box (45 cm width x 45cm depth x 50 cm height) with opaque polyvinyl plastic. Prior to the test, all mice were introduced to the test box for 5 min without objects. After the introduction period, mice were positioned into the open field box with two identical objects and allowed to explore for 5 min. The objects used in this experiment were wooden blocks with same size, but different shape. The time that mice spent on exploring each object was recorded (defined as the training session). 24h after the training session, mice were allowed to search the objects for 5 min, in which the familiar object used in the training session was replaced with a novel object. The time spent by the mice exploring the novel and the familiar objects was analyzed (defined as the test session) using the Ethovision XT software. The animals were regarded to be exploring when they were sniffing, biting, or facing the object. The objects and test box were cleaned with 75% ethanol after each session. Data are expressed in percentage terms of novel object recognition time% = total time spent with novel object/[total time spent with novel object + total time spent with familiar object] x 100.

Morris water maze test (MWMT)

The MWMT was performed as described.[51] The MWM is a white circular pool (150 cm in diameter and 50 cm in height) with four different inner cues on surface. The circular pool was filled with water and a nontoxic water-soluble white dye (20 ± 1°C) and the platform was submerged 1 cm below the surface of water so that it was invisible at water level. The pool was divided into four quadrants of equal area. A blue platform (9 cm in diameter and 15 cm in height) was centered in one of the four quadrants of the pool. The location of each swimming mouse, from the start position to the platform, was digitized by Ethovision XT software. The day before the experiment mice were subjected to swim training for 60 s in the absence of the platform. The mice were then given two trial sessions each day for four consecutive days, with an inter-trial interval of 15 min, and the escape latencies were recorded. This parameter was averaged for each session of trials and for each mouse. Once the mouse located the platform, it was permitted to remain on it for 10 s. If the mouse was unable to locate the platform within 60 s, it was placed on the platform for 10 s and then returned to its cage by the experimenter. On day 6, the probe trial test involved removing the platform from the pool and mice were allowed the cut-off time of 60 s.

Grooming

According to conventional protocol.[52] Mice were placed in autoclaved, empty standard cages and video recorded from the side for 15 min. The final 10 min were scored manually by two independent blinded, trained researchers for grooming behavior.

Marble burying

Marble burying was performed in a normal cage bottom filled with 3–4 cm of fresh, autoclaved wood chip bedding. The mice were first habituated to the cage for 10 min, and subsequently transferred to a holding cage while the bedding was leveled and 20 glass marbles (4 × 5) were placed on top. The mice were then returned to their own cage and removed after 10 min. The number of buried marbles (50% or more covered) was then recorded and photographed for reference and scored by an additional blinded researcher. A fresh cage was used for each mouse, and marble were soaked in 75% ethanol and dried in bedding in between tests.[53]

Social interaction

Each mouse was introduced to a fresh, empty, standard, autoclaved cage and allowed to habituate for 10 min before a novel mouse in age- and sex-matched was introduced to the cage for an additional 5 min for scoring of social activity. Two blinded, trained researchers scored videos for social behavior using the Ethovision XT software.[54]

Gastric emptying

Gastric emptying was performed on AAD- and NCD-fed mice. Prior to the experiment; mice were fasted for 12 h with free access to water. At the time of the experiment, mice were placed in separate clean cages and had access to pre-weighed food pellets for 1 h. The amount of food consumed was calculated based on food weight prior to and after access. Two hours later, food was removed, animals were sacrificed and their stomachs were removed. Gastric emptying was calculated according to the following formula: gastric emptying (%) = [1 - (weight of food in stomach/weight of food intake)] x 100.[55]

Bead latency

Distal colonic motility was measured by the bead latency test. Mice were anesthetized with isoflurane, and a lubricated, 2-mm diameter glass bead was inserted into the distal colon to a total depth of 2 cm from the anal margin using a fire-polished glass rod. After insertion of the bead, mice were isolated in clear plastic cages without food and water. The time required for expulsion of the glass bead was recorded, which was typically less than 15 min.[56]

Whole-gut transit time (WGTT)

Carmine red is a red dye that is not absorbed by the gut during digestion but excreted with other waste products. Solution of this dye was used to determine total GI transit time in AAD- and NCD-fed mice. A solution of carmine red (60 mg/mL) in 0.5% (v/v) carboxymethyl cellulose (key resources table) was administered by oral gavage. The volume of carmine red solution used for each animal was calculated based on animal weight (0.3 mg/g body weight). One hour after oral gavage, animals were monitored for the presence of carmine red in fecal pellets and the experiment was terminated after 8 h. Total GI transit time represented the time interval between the initiation of gavage and the first observance of carmine red in the stool.[57]

Feces water content

Fecal pellets excreted from mice were collected at 10:00 a.m. The weight of fecal pellets from each mouse were measured as A, the weight of feces after drying at 60°C for 24 h were measured as B. The water content was estimated by applying the following calculation method: Feces water content=(A−B)/A×100.[58]

Subdiaphragmatic vagotomy (sdVx)

2 weeks-old male mice were anesthetized using isoflurane (induction, 2% isoflurane with 1% oxygen; maintenance, 1% isoflurane with 1% oxygen). After adequate depth of anesthesia, expose the peritoneal cavity. The right and left vagus nerves were visualized along the esophagus below the diaphragm by a surgical microscope and cut using microscissors. Then the abdominal wall was closed using absorbable sutures and the skin was closed using surgical staples. For sham-operated mice, the vagus nerve was similarly exposed but not cut.[59] After one-week recovery, mice were started AAD-fed model, with 4 weeks consecutively AAD-fed and 2 weeks NCD-fed, at the age of 9 weeks, mice were conducted behavior tests and GI motility tests.

Evans Blue permeability assay

Mice were injected intravenous injection(i.v.) with a solution of 2% Evans Blue (w/v) (key resources table). 30 min after injection, mice were deeply anesthetized and perfused with 40 mL of Ca^{2+}/Mg^{2}+-free PBS. Brain tissue was isolated and pictured under black background.

Hematoxylin and eosin staining

The colon tissues were isolated, fixed in 4% PFA and embedded in paraffin. Sections were stained with hematoxylin and eosin by Servicebio (Wuhan, CN). Morphological changes in the stained sections were examined under a light microscope. For quantification, the sections were scored according to both histological and morphometric analysis, as previously described.[60]

QUANTIFICATION AND STATISTICAL ANALYSIS

Statistical analysis

The sample size chosen for our animal experiments in this study was estimated based on our prior experience of performing similar sets of experiments. All animal results were included, and no randomization method was applied. For all bar graphs, data were expressed as mean ± standard error of the mean (SEM). Statistical analysis was performed using unpaired Student's t-tests for two groups and one-way analysis of variance (ANOVA) or two-way ANOVA (GraphPad Prism Software) for multiple groups, with all data points (*https://www.graphpad.com/*) showing a normal distribution. To compare two non-parametric datasets, a Mann–Whitney U-test was employed. p values <0.05 were considered significant. The sample sizes (biological replicates), specific statistical tests, and the main effects of the statistical details of experiments can be found in each figure legend.